Journal of Magnetism and Magnetic Materials 473 (2019) 527–533

Contents lists available at ScienceDirect

Journal of Magnetism and Magnetic Materials

journal homepage: www.elsevier.com/locate/jmmm

Research articles

Development of a protocol to assess cell internalization and tissue uptake of magnetic nanoparticles by AC Biosusceptometry

Caio C. Quini[a,b,*,1], André G. Próspero[a,*,1], Bethany R. Kondiles[b], Lesley Chaboub[b], Matthew K. Hogan[b], Oswaldo Baffa[c], Andris F. Bakuzis[d], Philip J. Horner[b], José R.A. Miranda[a]

[a] Departamento de Física e Biofísica, Institute of Biosciences, Sao Paulo State University (Unesp), Botucatu, SP, Brazil
[b] Center for Neuroregeneration, Houston Methodist Research Institute, Houston, TX, United States
[c] Departamento de Física, Faculdade de Física, Ciências e Letras de Ribeirão Preto, University of Sao Paulo (USP), Ribeirão Preto, SP, Brazil
[d] Instituto de Física, Federal University of Goiás, Goiânia, GO, Brazil

A B S T R A C T

Several applications of nanoparticles rely on the internalization and accumulation of nanocarriers in specific cell compartments and tissues. However, the methods currently employed for characterizing such processes, although well described, are time consuming and do not provide *in vivo* information, which is a crucial barrier towards translational applications. Here, we hypothesize that the AC Biosusceptometry technique can be employed to assess cell internalization of magnetic nanoparticles, with possible applications in screening assays to track specific biomarkers and cell types. We tested a simpler and easier alternative to study cell internalization and tissue accumulation after perfusion. We utilized citrate coated, manganese ferrite nanoparticles and evaluated the internalization process in mouse macrophages cells (J774.A1) and in an embryonic neural stem cell culture (E14.5) after differentiation in astrocytes and neurons, to assess internalization specificity. Respecting the particles toxicity limits, we tested different concentration of particles, in different incubation times. Sequentially, we imaged the cell cultures to confirm internalization and nanoparticles localization, labeling nucleus and cell body to assure that the particles were inside the cells. Our results showed a linear behavior on internalization for different doses and an optimum incubation time of 2 h.

1. Introduction

Magnetic nanoparticles (MNPs) have been extensively employed on biomedical applications, either for diagnostic or therapeutic approaches [1,2]. Regardless their objective, one main step to be overcome is the cellular internalization process. There are many studies focused on understanding and surpassing this barrier. Successful, and possibly specific, internalization of particles by cells allows for cell tracking and separation, while it's translation to tissue samples can predict tissue growth, differentiated biodistribution, among other properties [3–5]. From the nanoparticle perspective, such quantification can assess toxicity, optimum incubation time and dose, and possibly internalization pathways.

However, the process for detecting and quantifying internalization is usually complicated, time consuming due to sample preparation, several steps in the protocol, and sometimes indirect, since it can depend on binding to fluorescent markers [6]. Thus, there is a logic demand for a technique that allows for simple, fast and non-destructive assessments without the need for sample preparation.

In order to access cell internalization of MNPs, some magnetometry techniques have been employed. Mazuel and co-workers studied the intracellular biodegradation of MNPs using magnetic methods such as magnetophoresis and vibrating sample magnetometry [7]. In this study, the authors claim the simplicity, low cost and high temporal resolution of the magnetophoresis technique to monitor the MNPs *in situ*. Also, they stated that magnetometry can access the magnetic moment of the MNPs and their size distribution. AC susceptometry and SQUID sensors also were employed in this task. The use of SQUID sensors allowed the magnetization saturation study of magnetic nanocubes in a lysosome-like environment [8]. In this way an AC susceptometer was used to study the Brownian and Néel relaxation of MNPs in live cells before and after the cell lysis indicating different relaxation mechanisms when the MNPs were within the cells [9].

The AC Biosusceptometry (ACB) is a biomagnetic system and has been employed on several studies to monitor magnetic nanoparticles in animal models *in vivo* [10] and also tissue samples, for biodistribution studies [11]. Here, we tested the sensitivity limits of the technique to employ the sys tem on an internalization assay. The main objective of this study was to create a protocol to assess cell internalization of magnetic nanoparticles by AC Biosusceptometry. In this study, we utilized Citrate-coated, superparamagnetic manganese ferrite nanoparticles (Cit-$MnFe_2O_4$) and tested the internalization process in

* Corresponding authors.
E-mail addresses: caioquini@gmail.com (C.C. Quini), andre.prospero@unesp.br (A.G. Próspero).
[1] Both authors contributed equally to the manuscript.

https://doi.org/10.1016/j.jmmm.2018.10.064
Received 24 June 2018; Received in revised form 15 September 2018; Accepted 13 October 2018
Available online 15 October 2018
0304-8853/

cultures of macrophages and neural-stem cells. The success of both protocols might enable the creation of an optimum device, which allows to perform evaluations on particles distribution, from cell culture, to tissue perfusion and further animal models. Compared with others systems, the ACB system has some equal characteristics as the high temporal resolution, low cost, portability and simplicity, but differently from the others, has potential be employed in the entire chain of MNPs biological applications, from the cell internalization to the *in vivo* monitoring.

2. Methods

2.1. AC Biosusceptometry

The ACB system works as a magnetic material detector. The system is composed by two identical excitation coils and two identical detector coils. One pair, composed by one detection and one excitation coil, is called detector system and is placed near the sample. The other pair, called reference, is placed far from the sample. Using a Lock-in amplifier and an audio amplifier, we applied an alternate current in the excitation coils, which in turn generate an AC magnetic field. Simultaneously, the detector coils are used to detect this magnetic field generated and a second one, generated by the magnetic material immersed in the first one. The detector and reference systems were built in a first order gradiometric configuration that enables the subtraction of the signal referent to the excitation field and the environmental noise, remaining only the signal from the field generated by the magnetic material excited. As described before, the system is sensitive to the material magnetic susceptibility and the distance between the sample and the sensor [12–14].

Here, we employed a new ACB configuration, in which the sample can be placed in the center of the detection coil, which increases substantially the sensitivity of the system. Fig. 1 illustrates the setup, indicating the differences, specially related to signal amplitude, when the sample is positioned on the surface of the sensor, as performed on previous studies of our group. Following our previous studies protocols, we built a calibration curve using different known concentrations of MNPs to calculate the mass of MNPs in the samples from the ACB system signal recorded [11].

2.2. Magnetic nanoparticles

We used a nanostructured manganese ferrite particle, coated with citric acid (Ci-$MnFe_2O_4$) and synthesized by coprecipitation method described previously by Branquinho et al. [15] and applied to kidney transit and perfusion studies on rats by Quini et al. [16]. Their physical size and Zeta potential were also described previously and reported to be 13 ± 4 nm and −27.8 mV at pH of 7.4, respectively [11,16]. Manganese ferrite was chosen as a tracer material due to its high magnetic susceptibility, aiming the optimization of the ACB detection system [11].

Before each experiment, we obtained a calibration curve using known concentrations of the nanoparticles for further quantification of all samples.

2.3. Experiments

We tested the internalization pattern for two different cell lines. First, with the objective of validating the protocol developed, we tested the internalization of Cit-$MnFe_2O_4$ by macrophages (mouse J774.A1 cells), under different doses and different incubation time. Sequentially, we assessed the internalization process promoted by embryonic (E14.5) neural stem cells. For this step, we tested only one concentration and two different time points.

Additionally, we developed a protocol for tissue perfusion of nanoparticles, followed by quantification of MNPs accumulation by ACB. All of these protocols were developed with the objective of creating a joint approach to study accumulation of nanoparticles in different stages of research, from *in vitro* studies to *in vivo* experiments.

2.4. Cell culture

J774.A1 mouse macrophages were kept on 10 mm well plates with high-glucose DMEM media (Dulbecco's Modified Eagle's Medium – 10% Fetal Bovine Serum) and incubated with various concentrations of nanoparticles and different incubation time. The purpose of this step was to define the detection limits for the ACB system, the incubation time necessary for the cells to internalize the particles and to test the ACB sensitivity to differentiate such levels of internalization.

We selected five different doses that would still remain below toxicity levels for the cells [17], with one control that received PBS (Phosphate Buffer Solution). We also tested different incubation times, considering the necessary time for these particles to be completely incorporated by the macrophages in an *in vivo* environment [11]. The dose ranged between 1.8 ug and 18 ug particles per cell in the well plate, while incubation time was 30 min, 1, 2 and 4 h. After plating, we waited for the cells to reach 75% confluence to start the MNP incubation protocol. After the respective time interval of each group, cells were moved to a volume controlled flask for further nanoparticle quantification by ACB. Fig. 2 illustrates this protocol.

Sequentially, we tested the specificity of the internalization process by inducing differentiation of the neural stem cells in culture plates before incubation with nanoparticles. The objective of this step was to identify a preferable cell type for internalization and to employ a joint approach between ACB and fluorescence imaging to assess internalization.

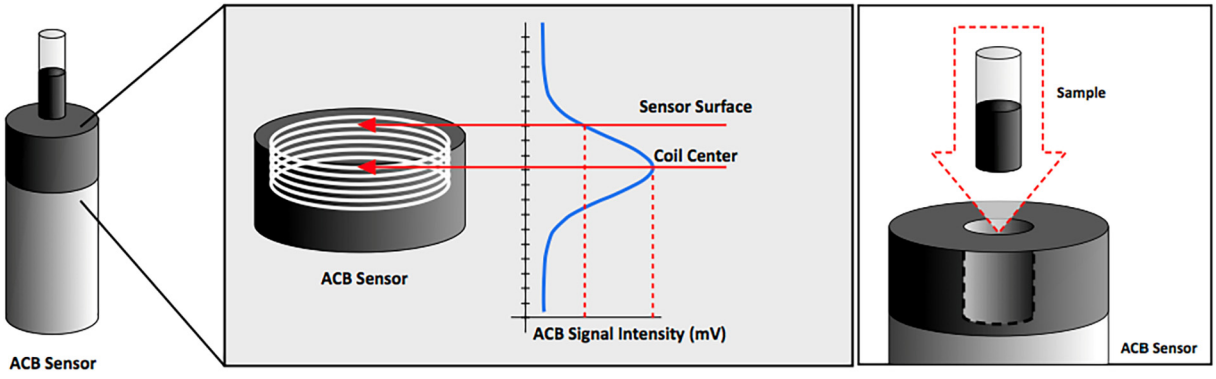

Fig. 1. Comparison between the previous ACB configuration, with the sample positioned on the surface of the sensor, and the new one, in which the sample can be placed in the center of detection coil, increasing the signal obtained from the sample.

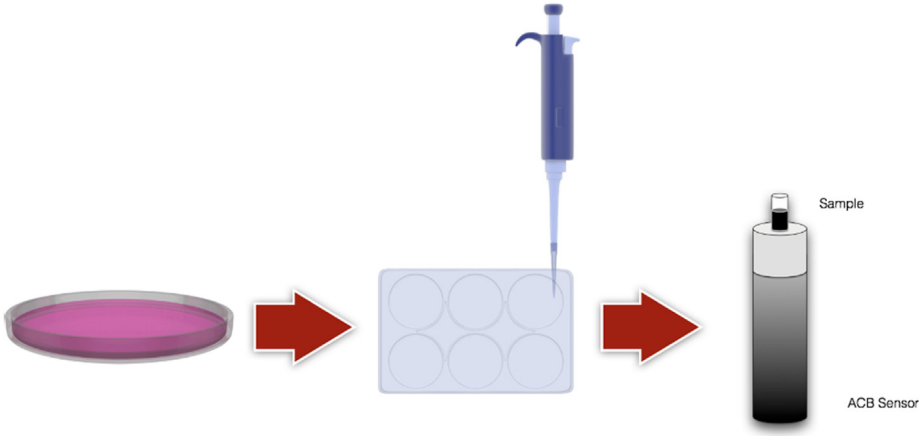

Fig. 2. Experimental setup, indicating steps of the experiment, from cell growth and plating, followed by incubation time (after cells reached 75% confluence in the cell plates) and further quantification of nanoparticles internalized by the cells using the AC Biosusceptometry system.

We induced differentiation of the neural stem cells into astrocytes and neurons by deprivation of Epidermal Growth Factor (EGF). As for the biomarkers chosen for the immunohistochemistry assay, we utilized DAPI (4′, 6-diamidino-2-phenylindole) as a nuclear marker, GFAP (Glial fibrillary acidic protein) for astrocytes.

Since neither neurons nor axons are expected to internalize as many particles as macrophages, we selected higher doses of nanoparticles in comparison to what was used for the previous step (1000, 2000, 3000 and 4000 particles per cell in the culture-plate) and defined a longer incubation time (24 h). We separated wells for imaging, to attest the low toxicity of the particles, the interaction between particles and the well-plates, for microscopy (transmission electron microscopy and confocal) and ACB quantification.

2.5. Tissue perfusion protocol

The next step was to test the accumulation of the nanocarriers on tissues of interest and to assess where in the tissue the MNPs would accumulate. Using the perfusion setup, showed in Fig. 6, we perfused *ex vivo* mouse brain slices sectioned at 400 µm, cultured with high glucose DMEM media and 1.5 mg/mL Cit-$MnFe_2O_4$. We tested this protocol with 6 tissue samples.

For the staining step, after perfusion, we fixed the tissue with 4% paraformaldehyde (PFA). Tissue was frozen, embedded, and sectioned at 40 µm on a cryostat. We utilized DAPI (4′, 6-diamidino-2-phenylindole) as a nuclear marker, VWF (Von Willebrand Factor) as a vasculature marker, S100B (**S100** calcium-binding protein B) for astrocytes and MAP2 (Microtubule-Associated Protein 2) for neurons.

3. Results and discussion

3.1. Macrophages

Fig. 7 shows the results after incubating the macrophage culture with Cit-$MnFe_2O_4$, for all doses and the uptake over time.

Table 1 presents the statistical results obtained from Fig. 4. In Table 1, is possible to see the differences between the time points for the same amount of particles and the differences between accumulation for same time point. In the first half-hour, there is no differences between the internalization for all the concentrations of particle. In the first hour, it is possible to see that greater amounts of particles showed greater internalization, which was expected, since there are more particles to interact with the cells. This pattern, besides some slight differences, repeats itself for all time points. Regarding the time points for the same amount of particles (columns), there is a pattern showing an increase of internalization along time. Besides the 1.8 ug and 3.6 ug

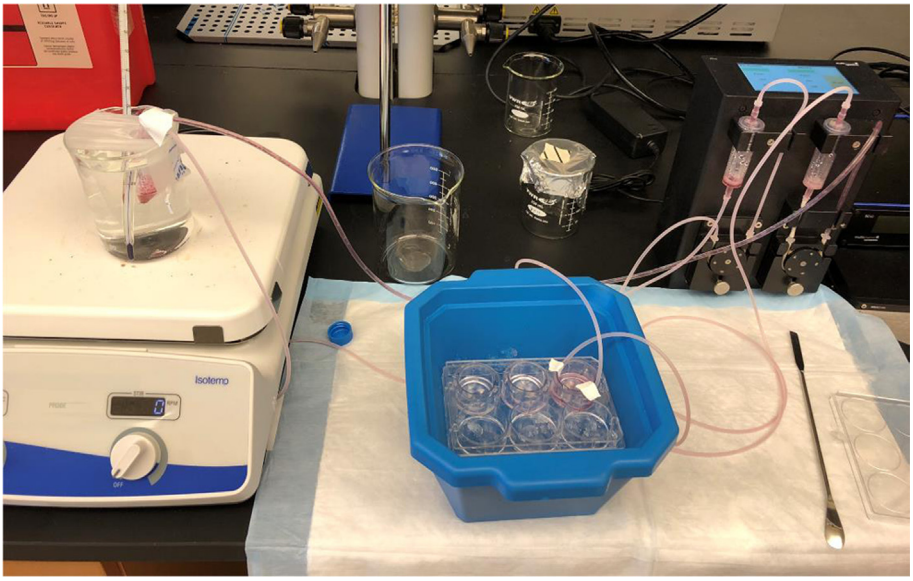

Fig. 3. Perfusion setup, showing the heated container, with the nanoparticles diluted in the cell media, the perfusion pump and the cell plate with the tissue samples.

Table 1
Incubation time and amount of particles statistical results.

Time (h)	PBS	1.8 ug	3.6 ug	5.4 ug	9.0 ug	18.0 ug
0.5	aA	aB	aA	aB	aB	aE
1	aA	aA	bA	bC	bC	bD
2	aA	bBC	cB	cC	cD	cE
4	aA	cB	cC	dC	dD	dE

*Different lowercase letters indicate a statistical difference ($p < 0,01$) between rows in the same column. Different uppercase letters indicate a statistical difference ($p < 0,01$) between columns in the same row.

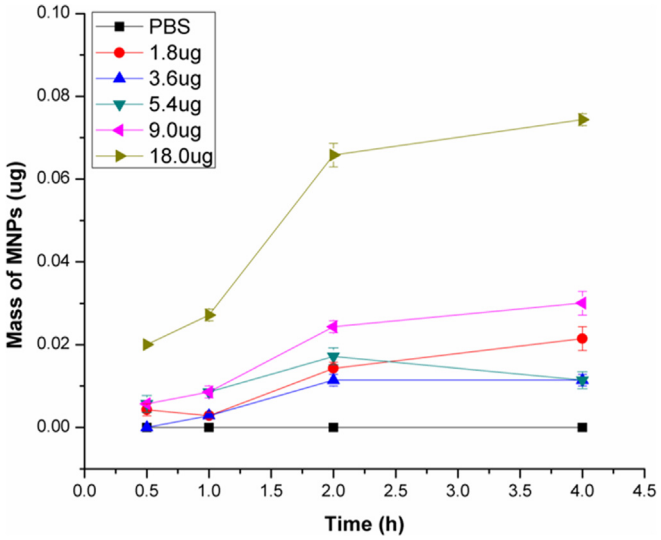

Fig. 4. Mass of MNPs calculated from the ACB signal intensity registered for each sample, with different doses administered and different incubation time.

MNPs groups, which presented no difference for some time points (i.e. 1.8 ug presented no difference up to the second hour and 3.6 ug presented no difference for the last two hours), all other quantities of particles showed difference between every time points. Although there is a difference between almost all time points, the increase in value observed from 1 h to 2 h is around one order of magnitude, while from 2 h to 4 h is much lower (Fig. 4). These results show a saturation pattern, indicating that, after the second hour, the cells did not internalize the same amount of particle as before. Our study suggests that there is low internalization after two hours of incubation, which may be an important consideration for other researchers before defining experimental protocols, making the procedure faster and objective.

3.2. Neural stem cells

After validating the internalization process with the macrophage culture, we tested the protocol in the neural stem cell culture, after differentiation into astrocytes and neurons. Fig. 8 shows one example of each group, which received different doses of particles. Bright field images were acquired on a Leica (See Fig. 5).

Fig. 6 shows images from the group that received 1000 particles per cell, stained for neurons, astrocytes and cell nuclei.

Fig. 6A shows the bright field image, which allows us to see the particles near what seems to be the nucleus of the cells, confirmed by the DAPI staining, in Fig. 6B. Fig. 6C shows GFAP staining for astrocytes and Fig. 9D shows all images combined. Both Fig. 6A and B indicate that particles were internalized, while the white arrows show that they were trapped near the nucleus. Fig. 7 shows the ACB signal obtained from the samples indicating the internalization of nanoparticles in each group. All data is presented in average ± standard deviation.

Fig. 7 suggests a linear behavior of the ACB signal in response to the changes in the doses of nanoparticles that each group received. Such behavior indicates that neither saturation of the internalization process nor toxicity levels were reached, even for higher doses. Additionally, the ACB system showed good sensitivity for all doses chosen.

These results indicate that the ACB protocol for MNPs quantification may be a useful tool for *in vitro* analysis, providing quantitative information over nanoparticles internalization, under different conditions and cell types.

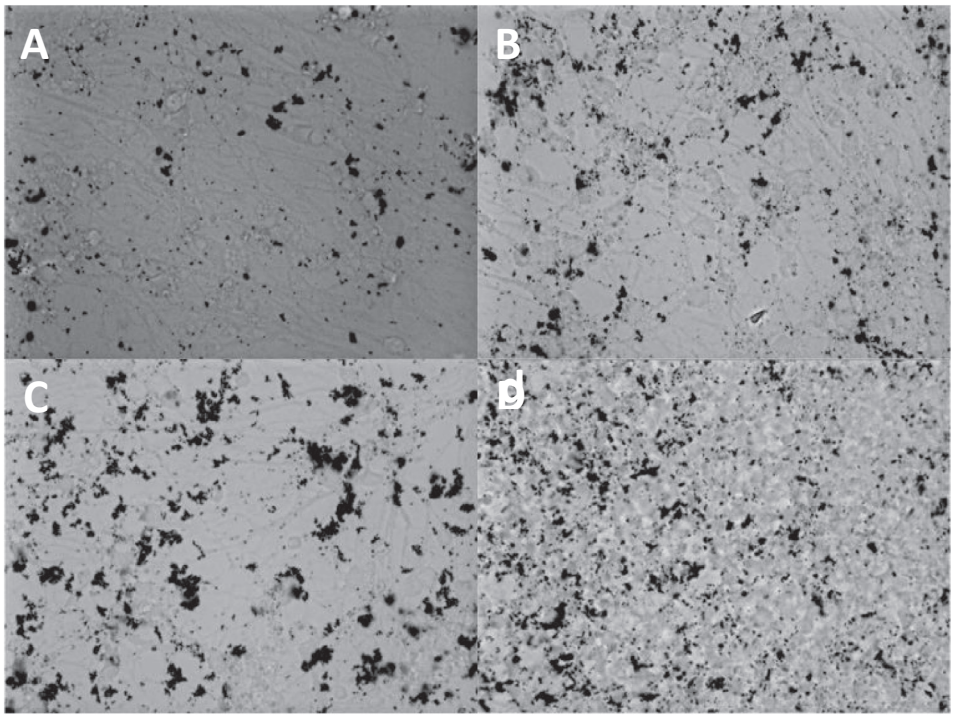

Fig. 5. Examples of each group, which received respectively 1000 (A), 2000 (B), 3000 (C) and 4000 (D) nanoparticles per cell.

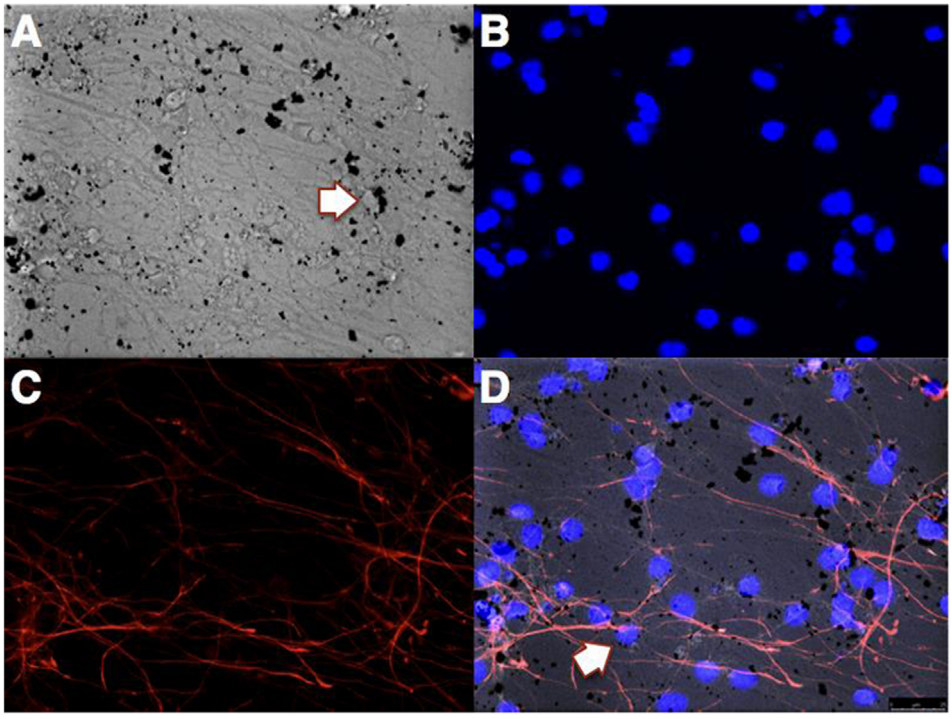

Fig. 6. Fluorescence images of the neural stem cell culture, after differentiation, showing bright field image in A, DAPI in B, GFAP in C and all combined in D.

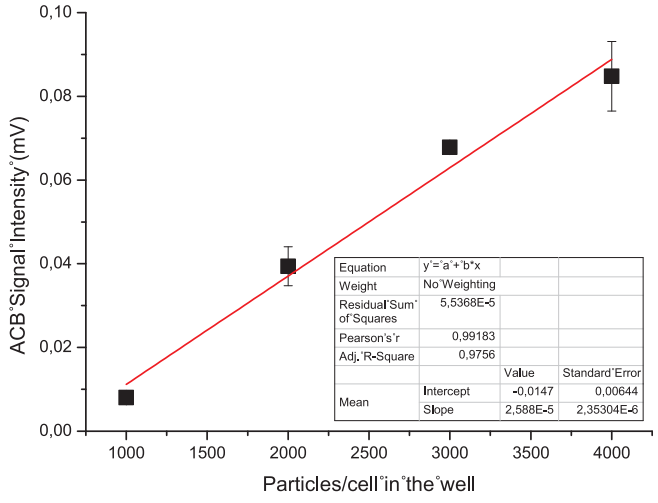

Fig. 7. ACB signal intensity obtained from each group, with different doses. Values are showed as average ± standard deviation.

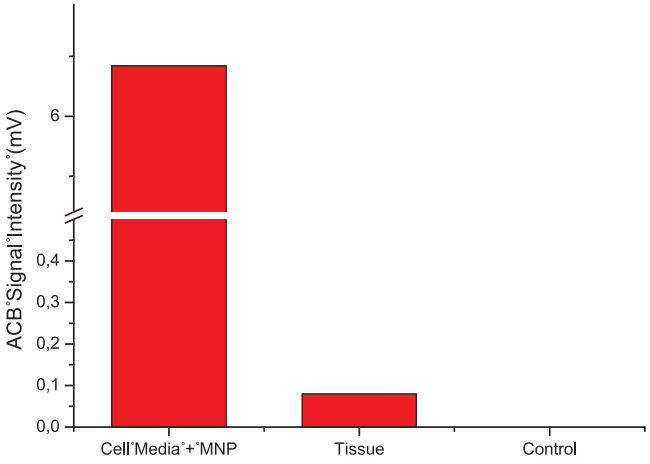

Fig. 9. ACB Signal acquired from control samples, tissues that received nanoparticles, and cell media with MNPs.

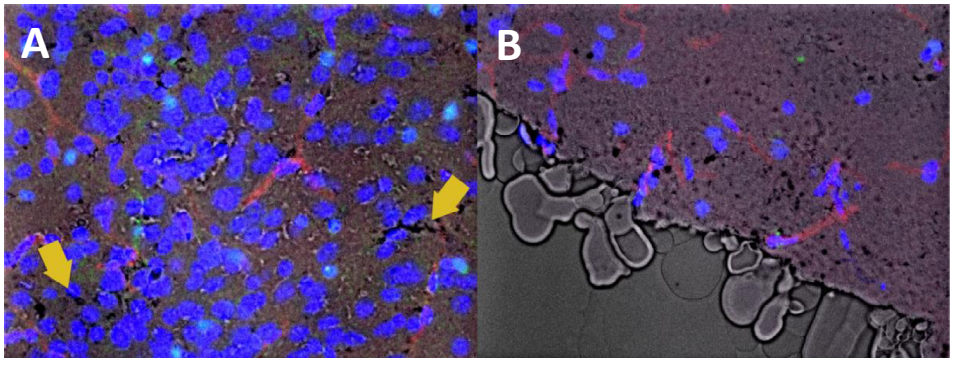

Fig. 8. Fluorescence images showing pools of nanoparticle accumulation (yellow arrows) with DAPI for nuclei staining, VWF for vasculature, S100B for astrocytes and MAP2 for neurons. **A** shows a region with pools of nanoparticles, accumulated in specific regions while **B** shows the edge of the tissue, which showed more accumulation. (For interpretation of the references to colour in this figure legend, the reader is referred to the web version of this article.)

Fig. 10. Tissue samples in the cell plate after perfusion of MNPs, indicating severe agglomeration, possibly flocculation, in the tissue and on the bottom of the cell plate.

3.3. Tissue uptake

For *ex vivo* experiments, we utilized the method described in Section 2.5 and illustrated in Fig. 3 to perfuse magnetic nanoparticles through unstained brain tissue. After 6 h of perfusion, all samples were washed 5 times with PBS and divided into 2 groups, imaging and ACB quantification. Tissue for imaging was fixed for an hour with 4% PFA prior to staining. Fig. 8 illustrates 2 regions of the tissue after perfusion, washing and staining protocol.

Fig. 8A shows few specific sites with large concentration of nanoparticles, indicated by the yellow arrows. These regions do not match the tissue vasculature, highlighted by the VWF stain. This indicates that particles are accumulating in the tissue and not just being passively trapped, as would be expected. Fig. 1B shows the edge of the sample, where we can observe an expected more intense accumulation process.

Fig. 9 shows the ACB signal of the samples that received the nanoparticles, in comparison with two other samples, namely control (tissue that received only cell media) and “cell media + MNP” (sample of media that was used in the experiment, with same concentration of nanoparticles).

In Fig. 9, we combined all of the samples in one vial and then performed the quantification in the ACB system. This step was necessary in order to reach the detection limit of the sensor. In addition to the detection limit of the sensor, the nanoparticles showed an expected loss of colloidal stability when in contact with cell media. This process by itself may interfere in the ACB signal obtained from the sample. Thus, these results suggest the use of new conjugation of MNPs to ensure the stability of the particles when in contact with biological media, such as cell media or blood. Fig. 10 shows an example of the particles accumulating in the tissue and the agglomeration process taking place at the edges of the tissue and on the bottom of the plate [18].

Interestingly, this pattern was not observed in the previous experiments with cells, which consisted of the same conjugation of nanoparticles (Cit-$MnFe_2O_4$), although in different concentrations. This data also suggests more experiments to better understand the stability of the nanoparticles in cell media and their relation with concentration. Optimized coating strategies should also increase the stability of the particles and thus enhance the accumulation process.

4. Conclusions

Over the last few years, MNPs cell internalization and tissue perfusion have been extensively explored and studied, drawing significant attention and growing as a research field. Determining the fate of the MNPs in the microscopic scale is an important step to increase their applicability and behavior in a biologic environment. Also, using the MNPs as a probe, it is possible to determine tissue growth, regeneration and degeneration, among other possibilities. There is still a need for new magnetic instrumentations to quantify cell internalization and retention of MNPs in perfused tissues. Here we created a protocol to measure cell internalization and tissue uptake of magnetic nanoparticles by AC Biosusceptometry with future application on tracking and quantification of specific biomarkers.

We successfully developed the entire protocol, with all necessary modifications in the perfusion system and the combined strategy to perform all the steps needed for the immunohistochemistry assay. This study was the first step of a new ACB application, and all the initial results suggest that the ACB system is a suitable tool to study cell internalization and tissue perfusion of MNP. Additionally, the data presented here suggests that the ACB system has the potential to be applied in a new research line based on tracking specific markers that will depend on the application of the study, based on the concept of biosensors for early diagnosis of different physiological processes.

Acknowledgements

The authors acknowledge the following funding institutions: Fundação de Amparo à Pesquisa do Estado de São Paulo (FAPESP), grant number 2015/14914-0 and 2017/00842-2. Brazilian Federal Agency for Support and Evaluation of Graduate Education within the Ministry of Education of Brazil (Capes).

References

[1] F. Wiekhorst, U. Steinhoff, D. Eberbeck, L. Trahms, Magnetorelaxometry assisting biomedical applications of magnetic nanoparticles, Pharm. Res. 29 (2012) 1189–1202.
[2] C. Sun, J.S. Lee, M. Zhang, Magnetic nanoparticles in MR imaging and drug delivery, Adv. Drug Deliv. Rev. 60 (2008) 1252–1265.
[3] S.E. Gratton, P.A. Ropp, P.D. Pohlhaus, J.C. Luft, V.J. Madden, M.E. Napier, J.M. DeSimone, The effect of particle design on cellular internalization pathways, Proc. Natl. Acad. Sci. U.S.A. 105 (2008) 11613–11618.
[4] M. Safi, J. Courtois, M. Seigneuret, H. Conjeaud, J.F. Berret, The effects of aggregation and protein corona on the cellular internalization of iron oxide nanoparticles, Biomaterials 32 (2011) 9353–9363.
[5] T.T. Sibov, L.A. Miyaki, J.B. Mamani, L.C. Marti, L.R. Sardinha, L.F. Pavon, D.M. Oliveira, W.H. Cardenas, L.F. Gamarra, Evaluation of umbilical cord mesenchymal stem cell labeling with superparamagnetic iron oxide nanoparticles coated with dextran and complexed with Poly-L-lysine, Einstein (Sao Paulo) 10 (2012) 180–188.
[6] M. Nakamura, K. Miyamoto, K. Hayashi, A. Awaad, M. Ochiai, K. Ishimura, Time-lapse fluorescence imaging and quantitative single cell and endosomal analysis of peritoneal macrophages using fluorescent organosilica nanoparticles, Nanomed. Nanotechnol. Biol. Med. 9 (2013) 274–283.
[7] F. Mazuel, A. Espinosa, N. Luciani, M. Reffay, R. Le Borgne, L. Motte, K. Desboeufs, A. Michel, T. Pellegrino, Y. Lalatonne, C. Wilhelm, Massive intracellular biodegradation of iron oxide nanoparticles evidenced magnetically at single-endosome and tissue levels, ACS Nano 10 (2016) 7627–7638.
[8] L. Lartigue, D. Alloyeau, J. Kolosnjaj-Tabi, Y. Javed, P. Guardia, A. Riedinger, C. Pechoux, T. Pellegrino, C. Wilhelm, F. Gazeau, Biodegradation of iron oxide nanocubes: high-resolution in situ monitoring, ACS Nano 7 (2013) 3939–3952.
[9] D. Soukup, S. Moise, E. Cespedes, J. Dobson, N.D. Telling, In situ measurement of magnetization relaxation of internalized nanoparticles in live cells, ACS Nano 9 (2015) 231–240.
[10] A.G. Prospero, C.C. Quini, A.F. Bakuzis, P. Fidelis-de-Oliveira, G.M. Moretto, F.P. Mello, M.F. Calabresi, R.V. Matos, E.A. Zandona, N. Zufelato, R.B. Oliveira, J.R. Miranda, Real-time in vivo monitoring of magnetic nanoparticles in the bloodstream by AC biosusceptometry, J. Nanobiotechnol. 15 (2017) 22.
[11] C.C. Quini, A.G. Prospero, M.F.F. Calabresi, G.M. Moretto, N. Zufelato, S. Krishnan, D.R. Pina, R.B. Oliveira, O. Baffa, A.F. Bakuzis, J.R.A. Miranda, Real-time liver uptake and biodistribution of magnetic nanoparticles determined by AC biosusceptometry, Nanomed. Nanotechnol. Biol. Med. 13 (2017) 1519–1529.
[12] O. Baffa, R.B. Oliveira, J.R. Miranda, L.E. Troncon, Analysis and development of AC biosusceptometer for orocaecal transit time measurements, Med. Biol. Eng. Comput.

33 (1995) 353–357.
[13] J.R.A. Miranda, R.B. Oliveira, N.M. Matsuda, O. Baffa, Susceptometric measurement of gastric-emptying, Int Congr Ser 988 (1992) 635–638.
[14] J.R.A. Miranda, R.B. Oliveira, P.L. Sousa, F.J.H. Braga, O. Baffa, A novel biomagnetic method to study gastric antral contractions, Phys. Med. Biol. 42 (1997) 1791–1799.
[15] L.C. Branquinho, M.S. Carriao, A.S. Costa, N. Zufelato, M.H. Sousa, R. Miotto, R. Ivkov, A.F. Bakuzis, Effect of magnetic dipolar interactions on nanoparticle heating efficiency: implications for cancer hyperthermia, Sci Rep-Uk 3 (2013).
[16] C.C. Quini, J.F. Matos, A.G. Próspero, M.F. Calabresi, N. Zufelato, A.F. Bakuzis, O. Baffa, J.R. Miranda, Renal perfusion evaluation by alternating current biosusceptometry of magnetic nanoparticles, J. Magn. Magn. Mater. (2014).
[17] S.L. O'Neal, W. Zheng, Manganese toxicity upon overexposure: a decade in review, Curr. Environ. Health Rep. 2 (2015) 315–328.
[18] L.C. Branquinho, M.S. Carriao, A.S. Costa, N. Zufelato, M.H. Sousa, R. Miotto, R. Ivkov, A.F. Bakuzis, Effect of magnetic dipolar interactions on nanoparticle heating efficiency: implications for cancer hyperthermia (vol 3, 2887, 2013), Sci Rep-Uk 4 (2014).